Supporting Information

Expanded Sandwich-like Heterostructure with Thin FeP Nanosheets@Graphene via Charge-Driven Self-Assembly as High-Performance Anodes for Sodium Ion Battery

Seungman Park [a, 1], *Dongwon Kim* [a, 1], *Myeongseok Jang* [a], *Taejin Hwang* [a], *Seon Jae Hwang* [a], *and Yuanzhe Piao* [a, b, *]

[a] Graduate School of Convergence Science and Technology, Seoul National University, 145 Gwanggyo-ro, Yeongtong-gu, Suwon-Si, Gyeonggi-do, 16229, Republic of Korea

[b] Advanced Institutes of Convergence Technology, 145 Gwanggyo-ro, Yeongtong-gu, Suwon-si, Gyeonggi-do, 16229, Republic of Korea

E-mail: parkat9@snu.ac.kr (Y. Piao)

[1] These authors contributed equally to this work.

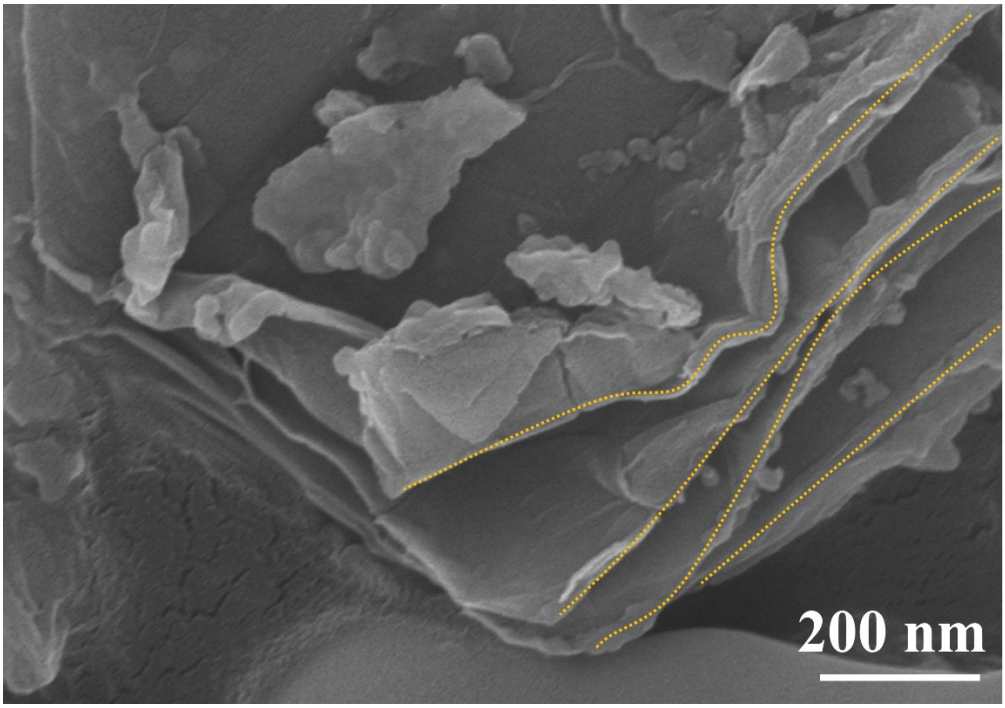

Fig. S1 High-resolution SEM image of expanded FeP NSs@rGO.

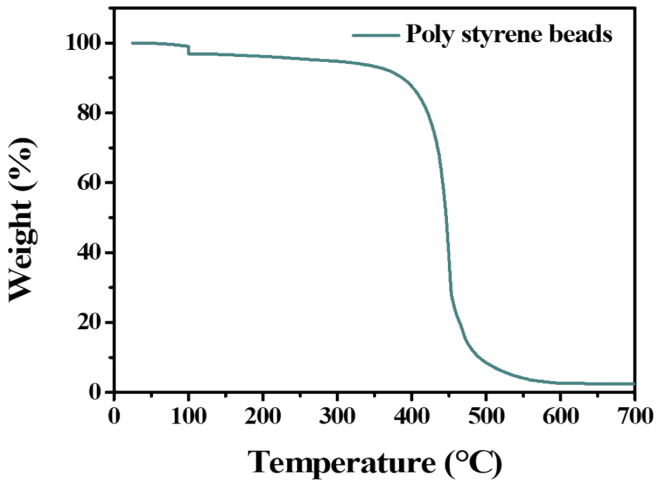

Fig. S2 TGA measurement of polystyrene beads (PSBs) with temperature range from 25 to 700 ˚C under Ar flow.

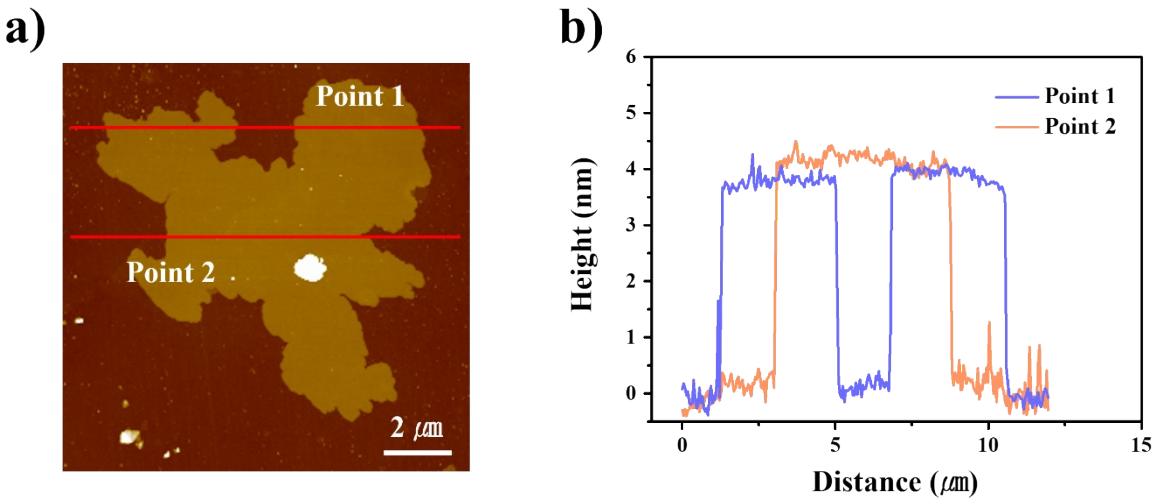

Fig. S3 Atomic force microscope (AFM) analysis of Fe-Tris NSs (a) and the corresponding plot of distance versus height (b).

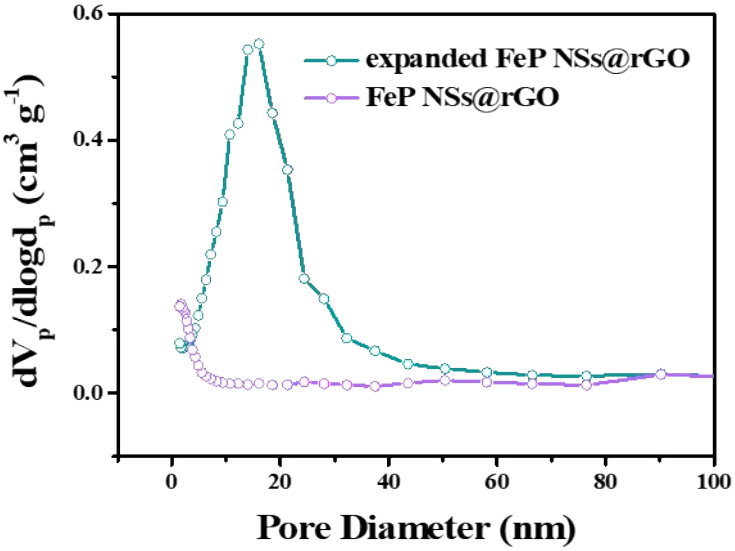

Fig. S4 Pore size distribution curves of expanded FeP NSs@rGO and FeP NSs@rGO samples.

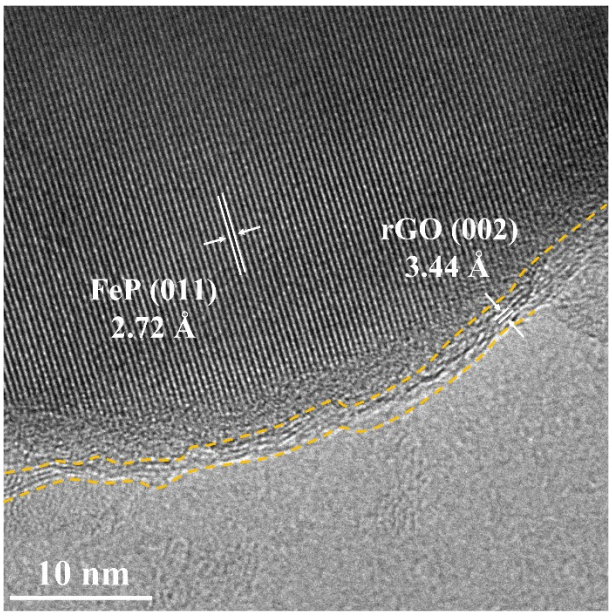

Fig. S5 HR-TEM image of expanded FeP NSs@rGO.

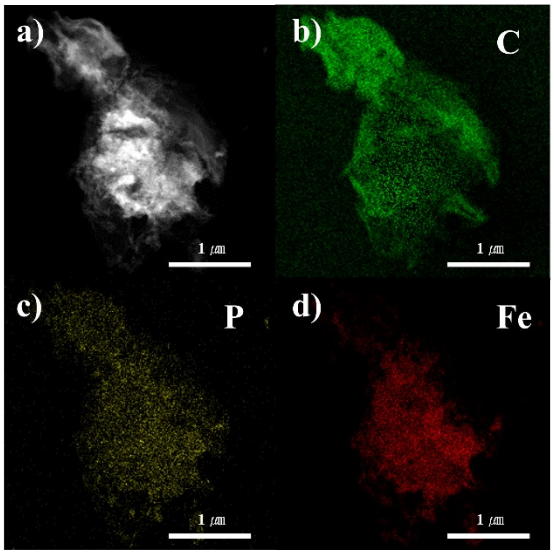

Fig. S6 EDS mapping images of FeP NSs@rGO.

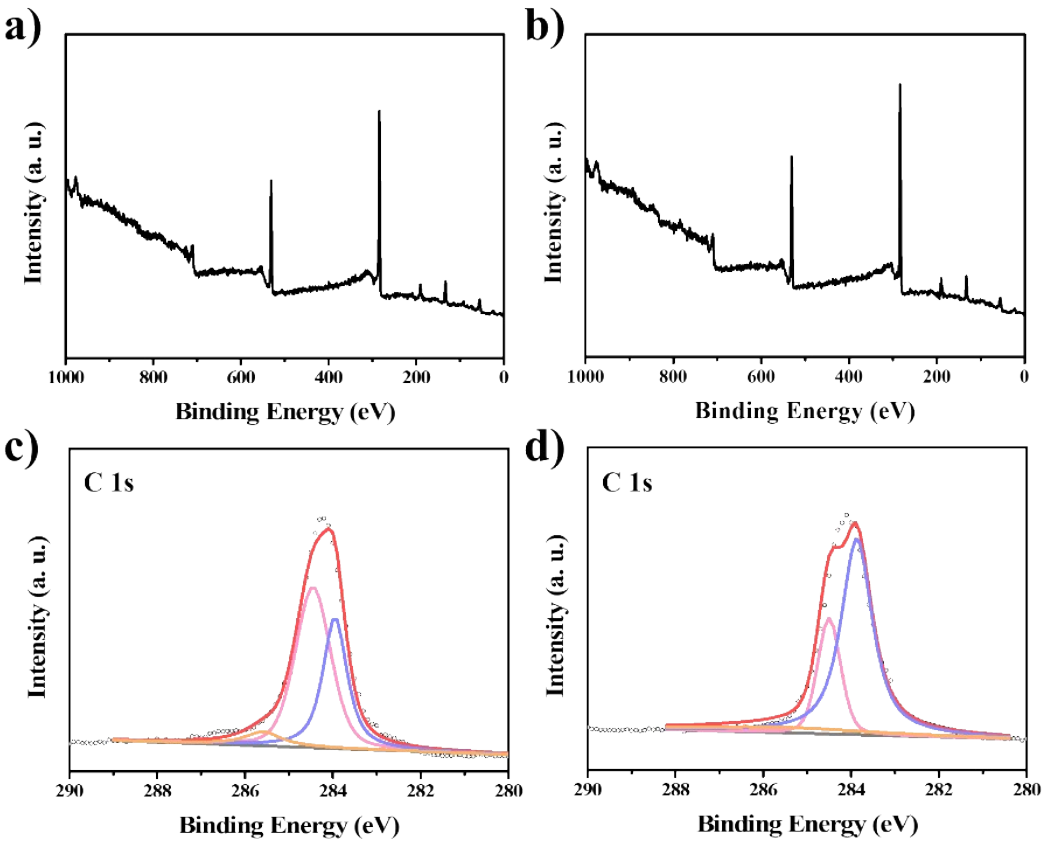

Fig. S7 XPS survey spectra of expanded FeP NSs@rGO (a), and FeP NSs@rGO (b); C 1s spectra for expanded FeP NSs@rGO (c), and FeP NSs@rGO (d).

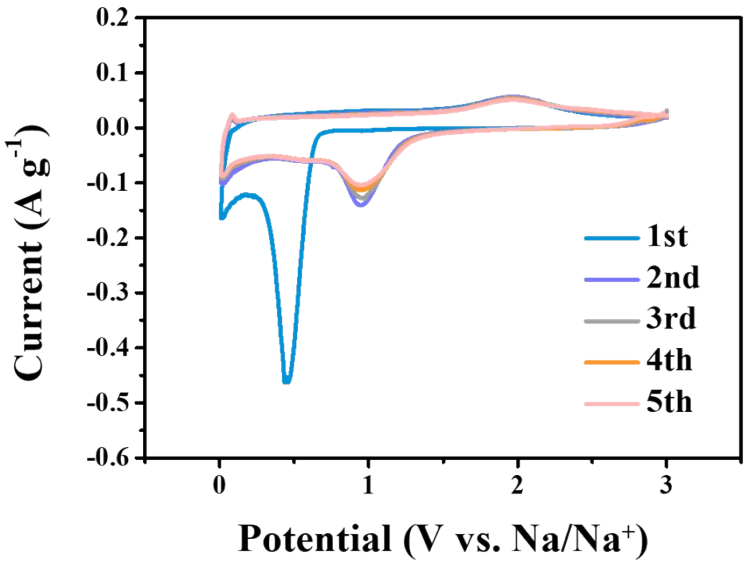

Fig. S8 CV curves of FeP NSs@rGO electrode of the first 5 cycles at a scan rate of 0.1 mV s^{-1} in the potential range of 0.001 ~ 3 V *vs*. Na/Na^+.

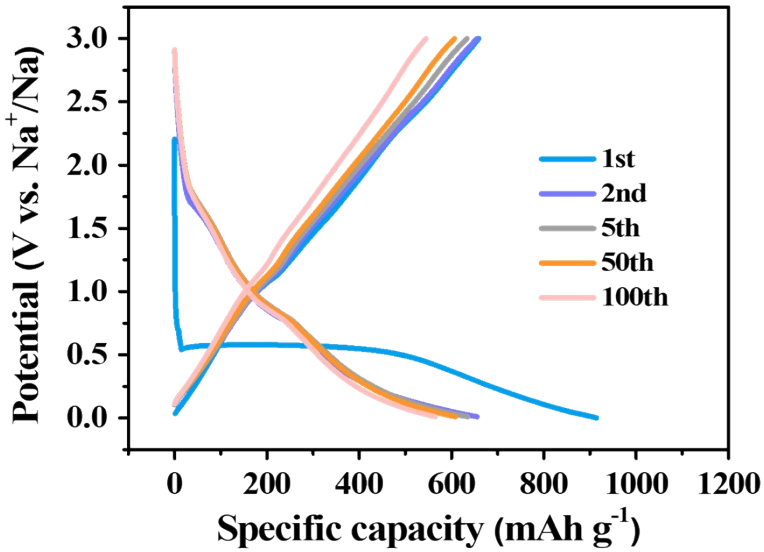

Fig. S9 Galvanostatic discharge-charge profiles of FeP NSs@rGO electrode of the first 100 cycles at a current density of 0.1 A g^{-1}.

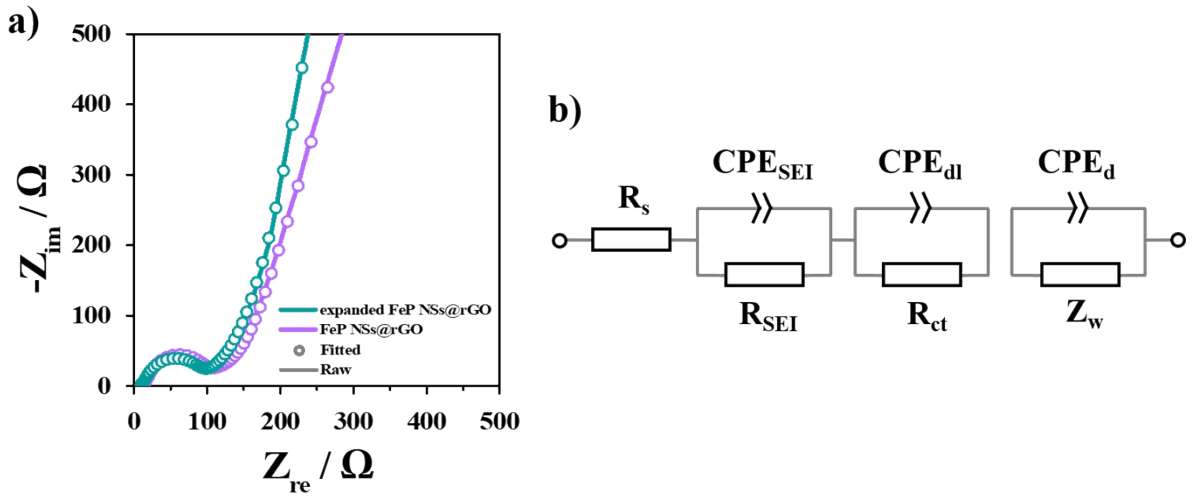

Fig. S10 Nyquist plot of expanded FeP NSs@rGO and FeP NSs@rGO electrodes (a), and corresponding equivalent circuits for expanded FeP NSs@rGO and FeP NSs@rGO electrodes (b).

Sample	Carbon content (wt %)
FeP NSs@rGO	5.03
expanded FeP NSs@rGO	5.37

Table S1 Elemental analysis of FeP NSs@rGO and expanded FeP NSs@rGO.

Samples	R_Ω / Ω·cm^{-2}	R_{SEI} / Ω·cm^{-2}	R_{ct} / Ω·cm^{-2}
expanded FeP NSs@rGO	**7.47 ± 0.19**	**10.02 ± 2.12**	**72.12 ± 1.34**
FeP NSs@rGO	**8.87 ± 0.23**	**12.98 ± 5.32**	**78.28 ± 5.24**

Table S2 The fitting values of the resistance components in the simplified equivalent circuit.

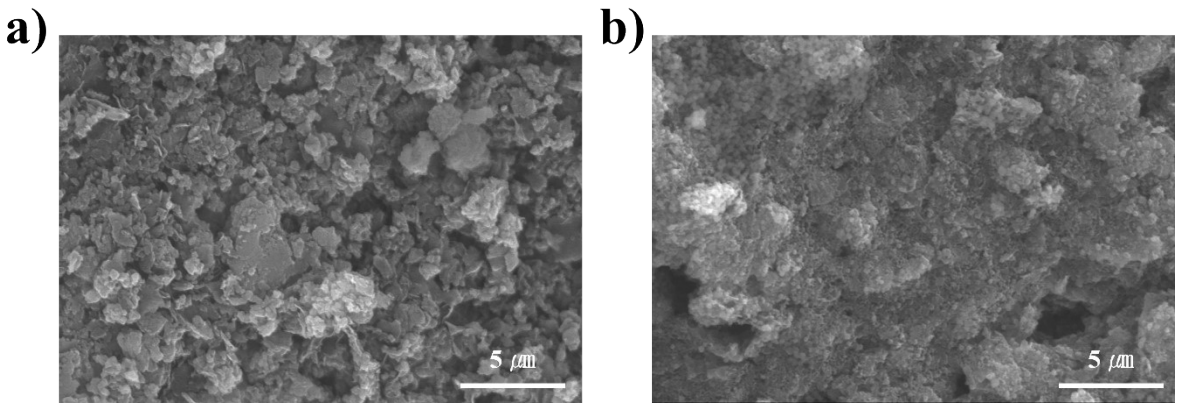

Fig. S11 SEM images of FeP NSs@rGO (a) and expanded FeP NSs@rGO (b) electrodes after 100 cycles at a current density of 1 A g^{-1}.

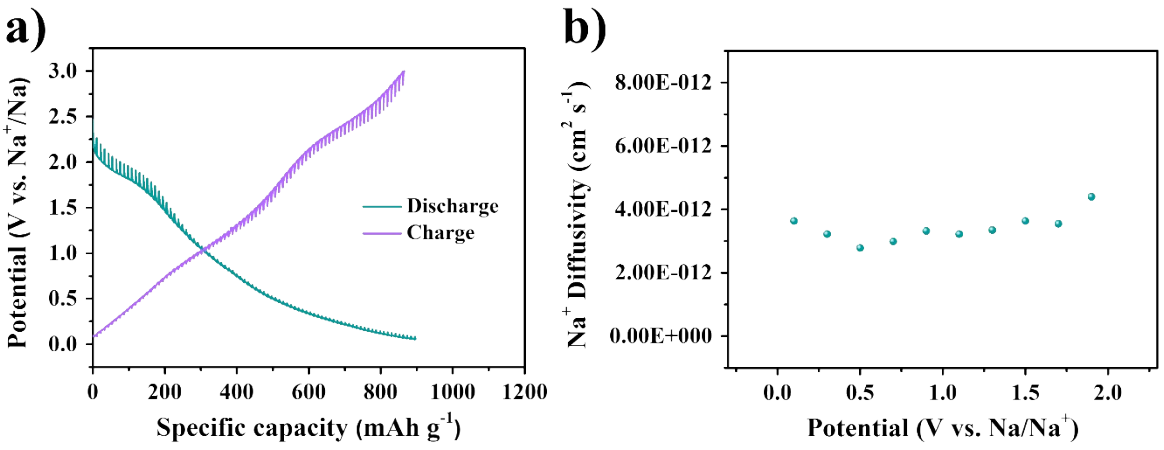

Fig. S12 The GITT curves (a) and the Na^+ diffusion coefficient (b) of expanded FeP NSs@rGO.

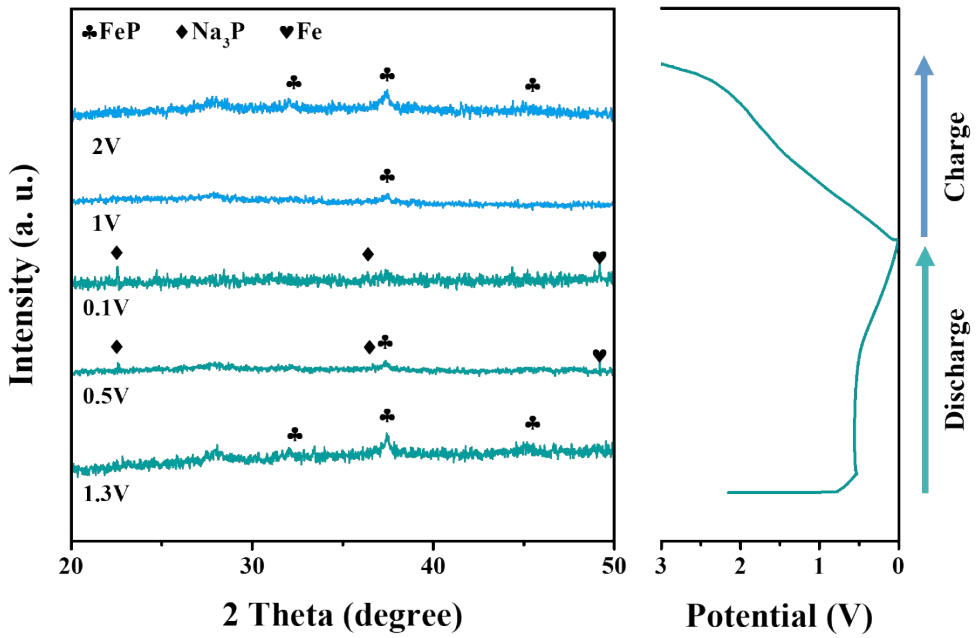

Fig. S13 Ex-situ XRD patterns of expanded FeP NSs@rGO anode with the corresponding galvanostatic discharge-charge profiles at a current density of 0.1 A g^{-1}.

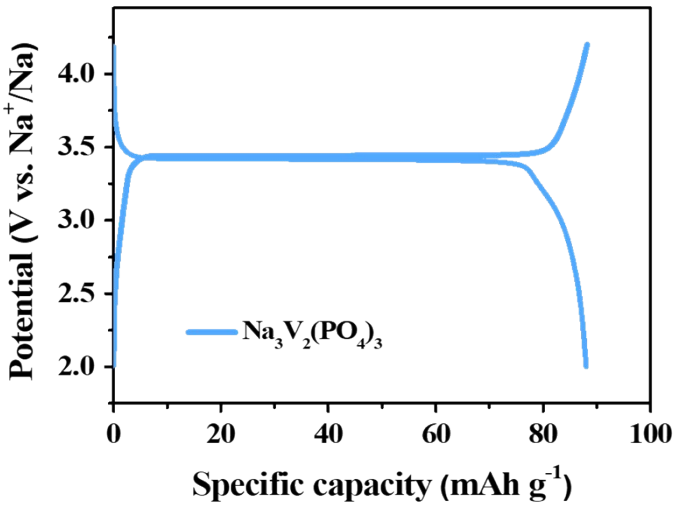

Fig. S14 Galvanostatic discharge-charge profiles of $Na_3V_2(PO_4)_3$ electrode at a current density of 0.1 A g^{-1}.

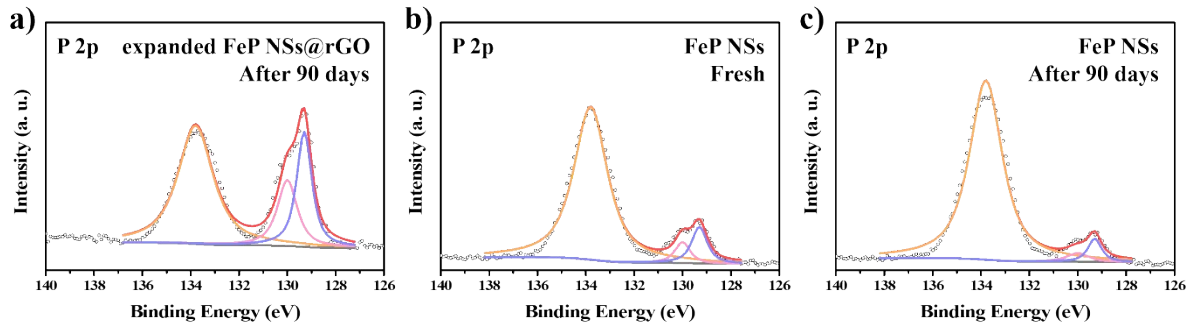

Fig. S15 XPS survey spectra of the air stability. P 2p spectra for expanded FeP NSs@rGO after exposure to the ambient atmosphere for 90 days (a), fresh FeP NSs (b), and FeP NSs after 90days (c).